Near-field control of optical bistability in a nanocavity

Damien Brissinger,[1] Benoit Cluzel,[1,*] Aurélien Coillet,[2] Colette Dumas,[1] Philippe Grelu,[2] and Frédérique de Fornel[1]
[1]*Groupe d'Optique de Champ Proche, Institut Carnot de Bourgogne (ICB),UMR CNRS 5209, Université de Bourgogne, 9, avenue A. Savary, BP 47870, 21078 Dijon, France*
[2]*Equipe Solitons, Lasers et Communications Optiques, Institut Carnot de Bourgogne (ICB), UMR CNRS 5209, Université de Bourgogne, 9, avenue A. Savary, BP 47870, 21078 Dijon, France*
(Received 27 January 2009; published 8 July 2009)

Dynamic control of the optical bistability of a nonlinear nanoresonator is shown to be achievable by modifying the resonance of the optical cavity with a dielectric near-field tip. It is experimentally demonstrated that the operating regime of the nanocavity can be switched between monostable and bistable regimes. Finally, an analytical model is proposed which provides an adequate description of the properties of the whole nonlinear optomechanical system.

DOI: 10.1103/PhysRevB.80.033103 PACS number(s): 42.65.Pc, 07.79.Fc, 42.70.Nq

Photonic crystal (PC) nanocavities have attracted a lot of attention over the last decade since they open innovative ways to manipulate light, which includes the slowing and the trapping of light,[1] quantum electrodynamics experiments,[2,3] and the enhancement of light-matter interactions.[4] Their ability to confine and enhance the electromagnetic field inside a very small volume is of great interest for nonlinear optics. Indeed, input power requirements, for instance the power threshold to reach optical bistability,[5–8] can be drastically reduced.

However, future applications of photonic nanocavities such as sensors,[9] modulators,[10] or emitters[11] will require the dynamical control of the optical resonance. This fundamental challenge has been addressed in the linear optical regime by several techniques, which include free-carrier injection,[12] thermal control,[13] integrated fluidics,[14] near-field probes,[15–17] or metallic probes.[18]

In this Brief Report, we address the dynamical control of a silicon nanocavity in the nonlinear regime by using a pure dielectric near-field tip. We experimentally demonstrate that the operation of the nanocavity can be switched between monostable and bistable regimes under the influence of the near-field tip. In the first part of this Brief Report, we present the linear and nonlinear optical properties of the nanocavity under study. In the second part, we experimentally prove the active control by the near-field tip of the bistable behavior of the nanocavity. Finally, in order to understand the whole nonlinear optomechanical system, we develop a Fabry-Perot (FP) model that takes into account the nonlinearity of the nanocavity as well as its near-field interaction with the near-field tip.

To begin with, we have studied several FP-like nanocavities etched in single mode silicon waveguides laid on a silicon-on-insulator substrate. Each cavity is composed of two photonic crystal mirrors designed to minimize losses[19] and improve cavity quality factor (Q) inside the cavity volume $[\sim 0.6(\lambda/n)^3]$. The fabrication process is detailed elsewhere.[20] Figure 1 shows a scanning electron microscope (SEM) view of the nanocavity under study. The nanocavity is characterized by using an end fire coupling technique. A transverse electrical (TE) polarized tunable laser is focused at the entrance facet of a silicon waveguide and all the light transmitted at the end of the waveguide is collected by an InGaAsP photodiode. In the preliminary, we quantify the light coupling efficiency in order to evaluate the power injected inside the nanocavity (P_{in}). This is done by measuring the power transmitted trough a cavityless waveguide with the same dimension and by taking Fresnel reflections into account.

We then recorded the transmitted spectrum of the nanocavity (Fig. 1). At low input power, the nanocavity resonance produces a Lorentzian-shaped peak with superimposed oscillations. These oscillations correspond to Fabry-Perot resonances between the cleaved facets of the silicon sample.[20] In order to determine the intrinsic characteristics of the Fabry-Perot nanocavity, i.e., the Bragg mirror reflectivity (R) and transmission (T), the cavity length (L_c), and its effective index (n_0), we fit the Airy function to the experimental spectrum (see at Fig. 1):

$$P_{out} = P_{in}\frac{T^2}{(1-R)^2 + 4R\sin^2(\phi)}, \tag{1}$$

where $\phi = \phi_{lin} = \frac{2\pi n_0 L_c}{\lambda}$ is the phase shift inside the nanocavity. The resonance wavelength (λ_r^0) is achieved as $\phi = 2m\pi$, with m as an integer.

The nanocavity, which is considered hereafter, resonates at a wavelength of $\lambda_r^0 = 1558.271$ nm, and fitting to Eq. (1) yields: $R = 0.999\,75$, $T = 0.000\,10$, $L_c = 550$ nm, and $n_0 = 2.833\,22$. These values are comparable to those reported elsewhere for comparable cavities.[19,20] The corresponding Q factor is $Q \sim 25\,000$.

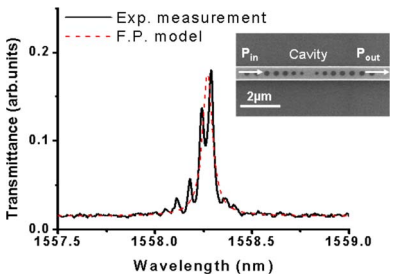

FIG. 1. (Color online) Experimental transmission spectrum through a high-Q ($\sim 25\,000$) small-volume $[\sim 0.6(\lambda/n)^3]$ Fabry-Perot-like nanocavity. The inset shows a SEM image of the cavity. The FP model prediction of the cavity resonance is superimposed in dashed line.

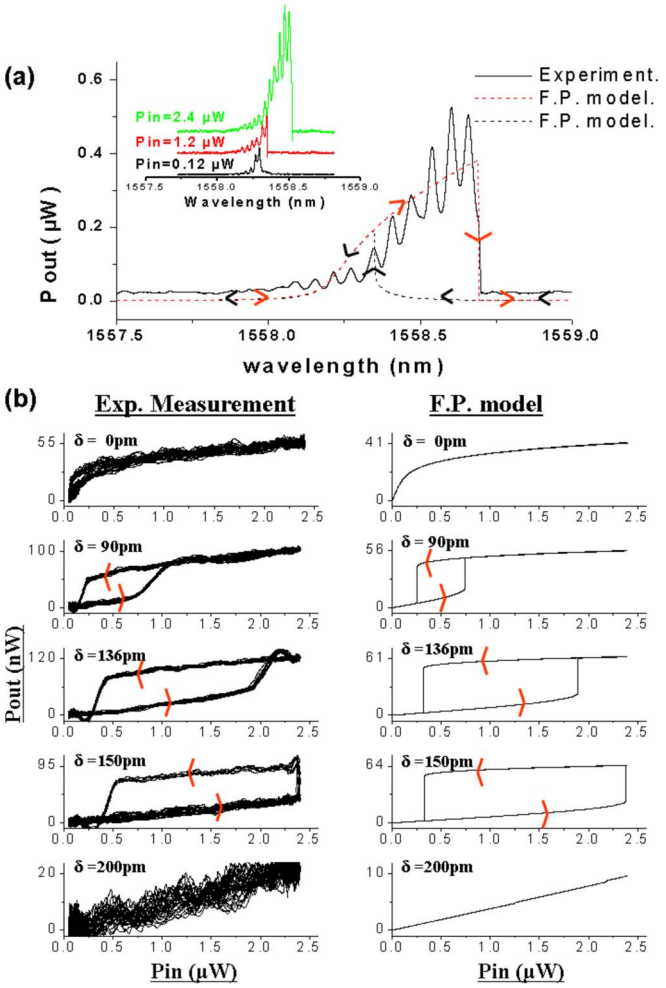

FIG. 2. (Color online) (a) Experimental transmission spectrum measured at maximum power (2.4 μW) through the Fabry-Perot-like nanocavity. The nonlinear Fabry-Perot model predictions of the spectrum are plotted in dashed line. The inset shows the evolution of the spectrum as a function of the injected power. (b) Experimental measurements and FP model predictions of the nanocavity hysteresis loops for few values of wavelength detuning δ.

As predicted and demonstrated,[7,21–23] a high-Q/small-V nanocavity allows reaching of the threshold of the nonlinear regime at a very low input power. In the case of the nanocavity studied in this work, a clear spectral signature of optical bistability is observed experimentally [inset of Fig. 2(a)] for an injected power as low as 1 μW. The bistable regime manifests itself in providing the spectral asymmetry and discontinuity[5] at the long-wavelength edge [Fig. 2(a)]. The very low power threshold reported here is in the actual range of thresholds recently reported in state-of-the-art nonlinear optical cavities.[21,22,24,25] In a silicon nanocavity, we expect that two-photon absorption (TPA) will produce a localized heating inside the cavity, resulting in a thermally induced nonlinear effect via the strong thermo-optic coefficient of silicon. This complex mechanism has been addressed by several authors.[22,24,26] The model used to fit the spectral recording confirms the bistability [Fig. 2(a)]. However, as the tunable laser only produces accurate wavelength sweeps from short to long wavelengths, the full spectral hysteresis loop could not be displayed experimentally.

We then modified our experimental setup in order to directly evidence bistability through the recording of the intensity transfer function, see Fig. 2(b), i.e., P_{out} as a function of P_{in}^8. As depicted in Fig. 3(a), the injected power P_{in} is modulated between 0 and 2.4 μW with an electro-optic modulator. We use a modulation frequency of 1 kHz, which is fast enough to reach thermal equilibrium in the bulk of the sample. Before light injection, 10% of the power is collected in order to get a reference proportional to P_{in}, and we visualize P_{out} as a function of P_{in} on an oscilloscope (Lecroy-Wavesurfer 4400XS). As shown in Fig. 2(b), the nanocavity exhibits monostable or bistable behavior depending on the operating wavelength (λ_w). We define the wavelength detuning (δ) as the difference between the operating wavelength and the resonance wavelength: $\delta=\lambda_w-\lambda_r^0$. The wavelength detuning δ should be positive in order to observe hysteresis loops. The larger the δ, the wider the hysteresis loop can be. However, the bistability threshold also increases with δ, and since the maximal injected power P_{in} is limited to 2.4 μW, hysteresis loops are not observed for $\delta > 150$ pm.

To model the experimental curves obtained in the nonlinear regime, the phase shift is modified to $\phi=\phi_{\text{lin}}+\phi_{\text{NL}}=\frac{2\pi n_0 L_c}{\lambda}+\frac{2\pi\Delta n(P_{\text{in}})L_c}{\lambda}$. We assumed instantaneous response of the nonlinear part of the refractive index $\Delta n(P_{\text{in}})$, which is consistent with the fact that the modulation frequency was in the kHz range whereas the thermo-optic effect inside the cavity should have response time below the microsecond range. The best fits of the experimental curves are obtained for Δn proportional to P_{in}^2. Such a quadratic behavior confirms that the nonlinear processes involved inside the nanocavity are mainly driven by TPA.[21,24] A comparison between the experimental and modeled intensity transfer functions is provided in Fig. 2(b), and presents a good agreement.

We have demonstrated without ambiguity that the nanocavity can operate in the nonlinear regime, yielding bistability at a very low threshold power. We now investigate the control over bistable operation which can be obtained by introducing a tip in the near-field of the nanocavity. As depicted in Fig. 3(a), we approach from the nanocavity surface a near-field tip that consists of a chemically etched monomode silica fiber optical with an apex of $\sim$200 nm. The tip position above the nanocavity is controlled thanks to a shear-force feedback and tridirectional piezoelectric stages. The tip is accurately positioned above the center of the nanocavity in light of different topographical images. We then modulate the tip height (h) above the nanocavity at low frequency (14 Hz) from $h=\sim 5$ nm to $h=200$ nm while we simultaneously record the intensity transfer functions of the nanocavity every millisecond. From this experiment, we extract hysteresis loops corresponding to different tip heights. Hysteresis loops measured at $h=200$, 140, 100, 50, and $\sim$5 nm are plotted in Fig. 3(b). The detuning in the absence of the tip is $\delta=300$ pm. One can observe that, for both large ($h > 140$ nm) and short ($h < 50$ nm) tip-cavity distances, the nanocavity operates in the monostable regime whereas for 50 nm $\leq h \leq$ 140 nm bistability is observed. The near-field tip clearly acts here as a mechanical switch between the

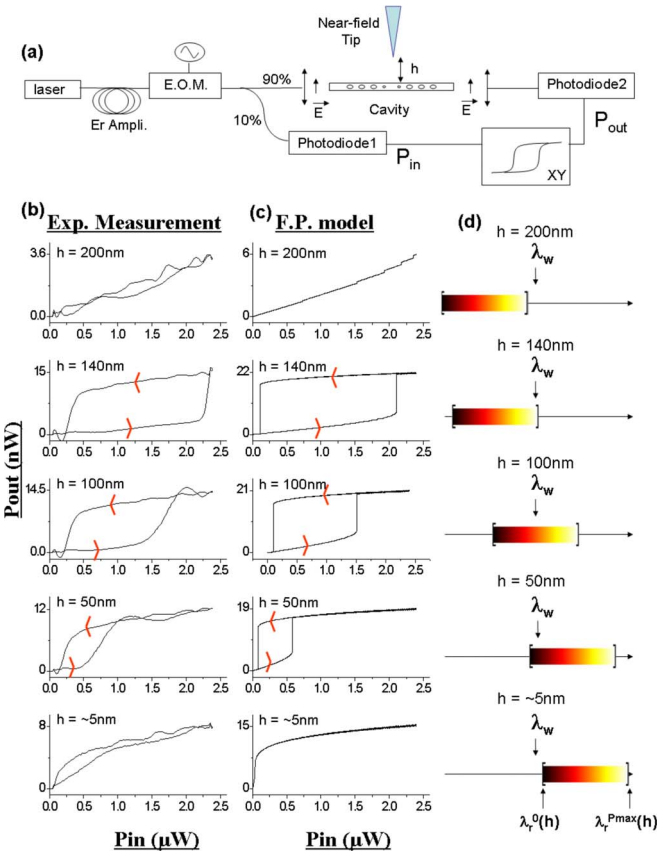

FIG. 3. (Color online) (a) Experimental setup used to measure the nanocavity hysteresis loops for various tip-cavity distances (h). Nanocavity hysteresis loops (b) measured and (c) predicted for various tip-cavity distances recorded at a constant detuning ($\delta = 300$ pm). (d) Schematic illustration of the bistable domain translation due to the tip-cavity interaction at a constant operating wavelength (λ_w).

monostable and the bistable regimes of the nanocavity.

We explain this behavior in light of the Fabry-Perot model. As recently reported,[27] a silica near-field tip with an apex dimension closed to 200 nm ($\sim\lambda/2n$) acts as an optical path modulator for the nanocavity since the vicinity of the near-field tip creates an additional phase shift (ϕ_{tip}). Consequently, the phase shift in the cavity becomes $\phi=\phi_{lin}+\phi_{NL}+\phi_{tip}=\frac{2\pi n_0 L_c}{\lambda}+\frac{2\pi\Delta n(P_{in})L_c}{\lambda}+\varphi_0\exp(\frac{-h}{a})$, where φ_0 is the maximal phase shift, close to the phase shift introduced when the near-field tip height is $h=5$ nm, a being the interaction length between the tip and the evanescent field of the cavity mode in air. φ_0 and a are directly evaluated by measuring the resonance redshift due to the near-field tip ($\Delta\lambda_{tip}=0.5$ nm in the reported experiment) at $h=5$ nm with a low P_{in}. The measured values are $a=80$ nm and $\varphi_0=1.210^{-3}$ rad. They are in the same range as those previously reported.[17,27] As shown in Fig. 3(c), the Fabry-Perot model predictions for the intensity transfer functions depending on the tip distance with the cavity, all obtained at the same wavelength detuning, are in very good agreement with experimental measurements.

Let us now analyze more systematically the measurements and the numerical predictions of Figs. 3(b) and 3(c).

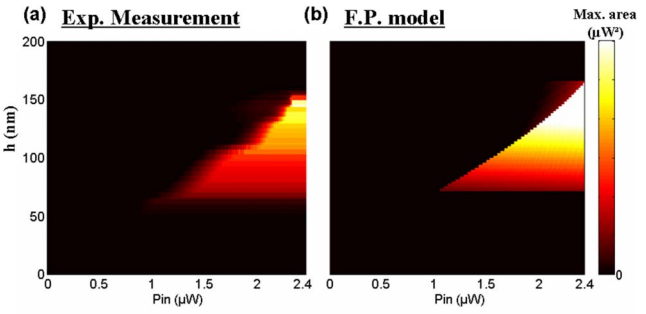

FIG. 4. (Color online) (a) Experimental and (b) simulated 2D diagrams of the hysteresis loop area variation as a function of the input power (P_{in}) and of the tip height (h) for a detuning of $\delta = 300$ pm. The representation allows a direct visualization of the (P_{in},h) sets that correspond to monostable or bistable regimes.

For a given tip height (h), the cavity is bistable if $\lambda_w \in [\lambda_r^0(h),\lambda_r^{Pmax}(h)]$, where $\lambda_r^0(h)$ and $\lambda_r^{Pmax}(h)$ are, respectively, the resonance wavelength at minimal and maximal power. In the measurement reported in Fig. 3, as long as λ_w is larger than $\lambda_r^{Pmax}(h)$, the cavity is monostable [$h = 200$ nm in Figs. 3(b) and 3(c)]. Reducing the near-field tip distance to the cavity, i.e., decreasing h, induces a simultaneous increase in $\lambda_r^0(h)$ and $\lambda_r^{Pmax}(h)$. Consequently, as depicted schematically in Fig. 3(d), approaching the near-field tip from the cavity surface results in a displacement of the interval $[\lambda_r^0(h),\lambda_r^{Pmax}(h)]$, the operating wavelength λ_w being unchanged. As soon as $\lambda_r^{Pmax}(h)$ becomes equal to λ_w, the cavity becomes bistable and a hysteresis loop appears ($h = 140$ nm). Then, as the near-field tip gets closer to the surface of the cavity, the detuning between λ_w and $\lambda_r^0(h)$ decreases, reducing the hysteresis loop aperture but the cavity remains bistable. When the tip is very close to the cavity surface ($h=\sim 5$ nm), λ_w becomes shorter than $\lambda_r^0(h)$, the wavelength detuning is negative, and the cavity becomes monostable. This demonstrates how a near-field tip can act on a nonlinear cavity as a mechanical actuator for switching between monostable and bistable operations. In addition, one can notice that controlling the tip height allows for fine tuning of the hysteresis loop. Finally, in order to provide a synthetic map of the operating regimes of the nanocavity as a function of the two active parameters P_{in} and h, we systematically measure the area defined by the hysteresis loop in function of P_{in} and h. We plot the two-dimensional (2D) diagram extracted from the experimental measurements in Fig. 4(a) and the numerical one obtained with the Fabry-Perot model in Fig. 4(b). A good agreement is achieved between the two diagrams. On these diagrams, two different regions are clearly visible. In one of them, the hysteresis area is zero and consequently the set (P_{in},h) makes the nanocavity operate in the monostable regime. In the other one, the hysteresis area is greater than zero and thus the set (P_{in},h) makes the nanocavity operate in the bistable regime. The frontiers at constant h between the different domains are directly defined by the interval $[\lambda_r^0(h),\lambda_r^{Pmax}(h)]$. The asymptotic frontier is the location of the bistability threshold of the nanocavity. In other words, those 2D diagrams allow for direct knowledge of the cavity operating regime in function of the input power and the tip height.

In conclusion, we have experimentally demonstrated that the optical bistability of a nonlinear solid-state nanoresonator can be efficiently controlled by using an optomechanical-near-field interaction. First, we presented the properties of the nonlinear nanocavity considered in this Brief Report. We then experimentally showed that a silica near-field tip can be used to control the nonlinear behavior of the studied nanocavity. Finally, in order to provide a clear understanding of the whole nonlinear optomechanical system reported here, we developed an analytical Fabry-Perot model that takes into account the nanocavity nonlinearities as well as the near-field interaction with the tip. To the best of our knowledge, this work proposes and demonstrates the feasibility of an innovative way to mechanically control the bistability of an optical system at nanometer scale.

The authors are grateful to Philippe Lalanne from Laboratoire Charles Fabry de l'Institut d'Optique for fruitful discussions. We also acknowledge David Peyrade from Laboratoire des Technologies de la Microélectronique for providing us the samples.

*benoit.cluzel@u-bourgogne.fr

[1] T. Tanabe, M. Notomi, E. Kuramochi, A. Shinya, and H. Taniyama, Nat. Photonics **1**, 49 (2007).
[2] K. Hennessy, A. Badolato, M. Winger, D. Gerace, M. Atatüre, S. Gulde, S. Fält, E. L. Hu, and A. Imamoglu, Nature (London) **445**, 896 (2007).
[3] T. Yoshie, A. Scherer, J. Hendrickson, G. Khitrova, H. M. Gibbs, G. Rupper, C. Ell, O. B. Shchekin, and D. G. Deppe, Nature (London) **432**, 200 (2004).
[4] M. Soljacic and J. D. Joannopoulos, Nature Mater. **3**, 211 (2004).
[5] H. M. Gibbs, *Optical Bistability* (Academic Press, Orlando, FL, 1985).
[6] A. R. Cowan and J. F. Young, Phys. Rev. E **68**, 046606 (2003).
[7] M. Soljacic, M. Ibanescu, S. G. Johnson, Y. Fink, and J. D. Joannopoulos, Phys. Rev. E **66**, 055601(R) (2002).
[8] G. Vienne, Y. Li, L. Tong, and Ph. Grelu, Opt. Lett. **33**, 1500 (2008).
[9] B. Schmidt, V. Almeida, C. Manolatou, S. Preble, and M. Lipson, Appl. Phys. Lett. **85**, 4854 (2004).
[10] I. Fushman, E. Waks, D. Englund, N. Stoltz, P. Petroff, and J. Vučković, Appl. Phys. Lett. **90**, 091118 (2007).
[11] H.-G. Park, S.-H. Kim, S.-H. Kwon, Y.-G. Ju, J.-K. Yang, J. H. Baek, S.-B. Kim, and Y.-H. Lee, Science **305**, 1444 (2004).
[12] V. R. Almeida, C. A. Barrios, R. C. Panepuci, and M. Lipson, Nature (London) **431**, 1081 (2004).
[13] H. M. H. Chong and R. M. De La Rue, IEEE Photon. Technol. Lett. **16**, 1528 (2004).
[14] U. Levy, K. Campbell, A. Groisman, S. Mookherja, and Y. Fainman, Appl. Phys. Lett. **88**, 111107 (2006).
[15] A. F. Koenderink, M. Kafesaki, B. C. Buchler, and V. Sandoghdar, Phys. Rev. Lett. **95**, 153904 (2005).
[16] I. Märki, M. Salt, and H. P. Herzig, Opt. Express **14**, 2969 (2006).
[17] L. Lalouat , B. Cluzel, P. Velha, E. Picard, D. Peyrade, J. P. Hugonin, P. Lalanne, E. Hadji, and F. de Fornel, Phys. Rev. B **76**, 041102(R) (2007).
[18] J. T. Robinson and M. Lipson, Phys. Rev. Lett. **100**, 043902 (2008).
[19] C. Sauvan, G. Lecamp, P. Lalanne, and J. P. Hugonin, Opt. Express **13**, 245 (2005).
[20] P. Velha, J. C. Rodier, P. Lalanne, J. P. Hugonin, D. Peyrade, E. Picard, T. Charvolin, and E. Hadji, Appl. Phys. Lett. **89**, 171121 (2006).
[21] P. E. Barclay, K. Srinivasan, and O. Painter, Opt. Express **13**, 801 (2005).
[22] M. Notomi, A. Shinya, S. Mitsugi, G. Kira, E. Kuramochi, and T. Tanabe, Opt. Express **13**, 2678 (2005).
[23] E. Weidner, S. Combrié, A. De Rossi, Q.-V. Tran, and S. Cassette, Appl. Phys. Lett. **90**, 101118 (2007).
[24] T. Uesugi, B. Song, T. Asano, and S. Noda, Opt. Express **14**, 377 (2006).
[25] S. Combrié A. De Rossi, Q. V. Tran, and H. Benisty, Opt. Lett. **33**, 1908 (2008).
[26] J. Bravo-Abad, A. Rodriguez, P. Bermel, S. G. Johnson, J. D. Joannopoulos, and M. Soljacic, Opt. Express **15**, 16161 (2007).
[27] B. Cluzel, L. Lalouat, P. Velha, E. Picard, D. Peyrade, J. C. Rodier, T. Charvolin, P. Lalanne, F. de Fornel, and E. Hadji, Opt. Express **16**, 279 (2008).